



Original Article

## Electronic structures of isoquercitrin and its pharmacokinetic exploration with Dengue virus 1 NS5 methyl transferase

Afaf S Alwabli\*

Biological Sciences Department, College of Science &amp; Arts, Rabigh Campus, King Abdulaziz University, Jeddah, Saudi Arabia



### Article Info

### Abstract



Ar tory:

Received: October 25, 2024

Accepted: January 24, 2025

Published: February 28, 2025

Use your device to scan and read the article online



An enzyme called dengue virus (DENV) non-structural protein 5 (NS5) methyltransferase (MTase) aids in the virus's replication by encasing viral RNA. Here, we report on the impact of the dengue virus (DENV) protein NS5 methyltransferase domain (NS5-MTase). This study investigates the structural, electronic, and biological properties of isoquercitrin using Density Functional Theory (DFT). Frontier molecular orbital energies were evaluated to assess the reactivity of the compounds, while molecular electrostatic potential mapping provided insights into charge distribution. In-silico ADME and toxicity analyses were conducted to determine the drug-likeness and safety profiles of the compound. Molecular docking simulations examined the binding interactions between Isoquercitrin and its target protein. To evaluate the potential of Isoquercitrin as a drug candidate, aspects such as absorption, distribution, metabolism, excretion, toxicity (ADMET), drug-likeness, and compound accessibility were analyzed. The ADME and toxicity results revealed promising drug-like properties and low toxicity, underscoring the compound's therapeutic potential.

**Keywords:** Dengue virus, MTase, Density functional theory, ADMET, Molecular docking.

### 1. Introduction

The family Flaviviridae comprises at least 70 viral species that are feasted by mosquitoes & ticks. Some of these viruses cause human diseases, such as yellow fever virus, dengue virus, West Nile virus, & Japanese encephalitis virus. About 400 million cases of dengue each year worldwide, making it the most common virus to spread through mosquitoes [1]. One of the four serotypes of the dengue virus 1-4 can cause flu-like symptoms & fever, or it might develop into dengue hemorrhagic fever or dengue shock syndrome, which are more severe forms of the virus. If a person recovers from an infection with one dengue serotype & then contracts another serotype, the likelihood of developing more severe hemorrhagic fever increases [2]. Currently, there are no antiviral medications to treat flavivirus infections, & there is no vaccination to guard against serious illnesses brought on through any of the DENV serotypes [3]. There are around 11,000 nucleotides in the DENV RNA genome. Its 5' end has a type I RNA cap (m7GpppAmG), & its 3' end lacks a poly-A tail. The genome codes for seven non-structural proteins such as non-structural 1 (NS1), non-structural 2 (NS2A), non-structural 2B (NS2B), non-structural 3 (NS3), non-structural 4A (NS4A), non-structural 4B (NS4B), & non-structural 5 (NS5) as well as three structural proteins (capsid,

membrane, & envelope protein). Mid the DENV serotypes & the Flavivirus genus, NS5 is the largest (104 kDa) & most conserved non-structural protein. In the viral replication complex, originating in the perinuclear endoplasmic reticulum of the infected cell, NS5 is linked to several viral & cellular proteins throughout the viral lifecycle [4]. NS5 is the largest domain containing two central regions that are the N terminal region with methyltransferase, which covers the three activities required for cap synthesis (guanylyltransferase, guanine-N7-methyltransferase, & nucleoside-2'O-methyltransferase) while C terminal domain RNA-dependent RNA polymerase that executes de novo RNA synthesis [5,6]. Since the NS5 protein is vital for flavivirus replication, viral RNA methylation, RNA polymerization, & host immune system evasion, it is a prospective therapeutic target. Creating a drug targeting all flaviviruses may be practicable because the NS5 protein's enzymatic centers are highly conserved across the Flaviviridae.

Isoquercitrin belongs to the class of chemical compounds known as flavonoids. It is quercetin's 3-O-glucoside. Many plant species, such as *Rheum nobile* and *Mangifera indica*, can yield Isoquercitrin. *Annona squamosa*, *Camellia sinensis*, and *Vestia foetida* leaves contain it [7]. Isoquercitrin demonstrated potent suppression of the Zika virus by blocking its internalization into host cells and

\* Corresponding author.

E-mail address: [aalwabli@kau.edu.sa](mailto:aalwabli@kau.edu.sa) (Afaf S Alwabli).Doi: <http://dx.doi.org/10.14715/cmb/2025.71.2.16>

interfering with its entry mechanism.

Here, our main objective is to study the structures followed by chemical reactivity (electrophilic & nucleophilic regions) of the isoquercitrin compound using density functional theory (DFT) and evaluate the drug-likeness potential of Isoquercitrin using ADMET analysis. Furthermore, the binding affinities and interactions of Isoquercitrin with the target proteins will be investigated using molecular docking.

## 2. Methods and Materials

### 2.1. Sequence alignment and domain organization

The FASTA format of amino acid sequences of NS5 methyltransferase domain of DENV (1-269 amino acid) was applied for alignment and domain organization analysis. For domain organization use the available bioinformatics tool Prosite (<https://prosite.expasy.org/>) program. Similarly, we also draw a model of predicted features with expected binding sites in the domain. Domain organization can be determined using tools like InterPro, Pfam, or which help to identify and annotate domains in protein sequences.

### 2.2. Density Functional Theory (DFT)

Computational molecular modeling tools serve as invaluable resources in analyzing the physical and chemical characteristics of molecules. These tools enable researchers to explore intricate details about molecular structures, reactivity, and interactions, providing insights critical to fields such as chemistry, biology, and materials science [8-10]. Ref Among these techniques, DFT calculations are particularly noteworthy for their ability to yield precise data concerning both the structural and electronic properties of compounds. In the present study, the molecular geometry of isoquercitrin was optimized to obtain a stable configuration by employing Gaussian 16 software [11]. The optimization was carried out using the B3LYP hybrid functional, a widely recognized method for balancing computational efficiency and accuracy, along with the 6-31G basis set applied to all atoms [12,13]. The initial geometry of the species was modeled using GaussView 6.1[14].

### 2.3. ADMET 2.0

In-silico ADME screening utilizes computational methods to predict the pharmacokinetic properties of drug candidates, focusing on absorption, distribution, metabolism, and excretion [15]. The ADMET 2.0 online platform (<https://admetmesh.scbdd.com>) a free online cheminformatics tool was used to predict the potential drug property and to evaluate the pharmacokinetic profile of selected compounds [16]. The criteria based on Lipinski's rule of five include the compound that has less than 500 g/mol molecular weight; the compound that has less than 3 hydrogen-bond donors; less than 12 hydrogen-bond acceptors; less than 5 partition coefficient (log P) value and the compound with less than 12 number of rotatable bonds.

### 2.4 Molecular docking analysis

Molecular docking is one of the popular methods used for structure-based virtual screening [17]. The docking scores reflect favorable predicted poses of ligands which can vary depending on the algorithms used [18]. By predicting the molecular interaction between target and ligand,

docking studies save us time, energy and resources and in turn accelerate the process of drug development. The PDB file of dengue viral proteins, Dengue virus 1 NS5 Methyl transferase (5IKM) was retrieved from the molecular database RCSB (Research Collaboratory for Structural Bioinformatics). The associated ligand molecules and water molecules were removed using AutoDock-Tools (ADT) [19]. The preparation of target protein was done using AutoDock tools where hydrogen atoms were added at unfulfilled valencies to correct partial charges and merging of polar bonds was carried out. Visualization of ligand-protein interactions and docked poses was performed using the Biovia Discovery Studio Visualizer 2021 [20].

### 2.4. Statistical analysis

The statistical analyses in this study were conducted using advanced computational methods to evaluate the pharmacokinetic properties and interactions of Isoquercitrin with the Dengue virus NS5 methyltransferase. The Density Functional Theory (DFT) was employed to optimize the molecular geometry of Isoquercitrin, allowing for a detailed investigation of its electronic structure, including frontier molecular orbitals (HOMO and LUMO) and their energy gap, which was found to be 3.63 eV. This analysis provided insights into the compound's reactivity and stability. Additionally, in-silico ADME (Absorption, Distribution, Metabolism, and Excretion) screening was performed using the ADMET 2.0 platform, assessing parameters such as Caco-2 permeability and human intestinal absorption, which indicated promising drug-like characteristics. Molecular docking simulations further elucidated the binding affinities between Isoquercitrin and its target protein, highlighting its potential as a therapeutic agent against dengue virus infections. The results collectively underscore the significance of Isoquercitrin's structural and electronic properties in drug development processes.

## 3. Results

### 3.1. Sequence alignment & domain arrangement

The alignment of dengue NS5 methyltransferase domain was done by using bioinformatics tool CLUSTAL program (<http://www.ebi.ac.uk>). Here we identify the prediction of features. We highlighted the domain site in red color on the above region of align sequence and binding amino acid with specific position in green color in the below region of the align sequence (Figure 1A). Further, we draw a model with predicted features of the protein. Mostly we found that mRNA cap-binding site with K, F, E, R, amino acid on position 17, 28, 153, 214 in the sequence. S-adenosyl-L-methionine binding site with S, G, T, T, amino acid on position 59, 89, 107, 134. The binding site of Essential for 2'-O-methyltransferase activity with K, E, E with position 64, 183 and 219. mRNA cap binding; via carbonyl oxygen is located on 20 positions with L. The conserved motifs are boxed in pink colors, and the name of each amino acid in green box and position of amino acid in the sequence with yellowish color. The result reveals that the three major sites such as mRNA cap binding, S-adenosyl-L-methionine, Essential for 2'-O-methyltransferase activity, and mRNA cap binding; via carbonyl oxygen (Figure 1B). Similarly, we also identified conserved domain (5-266 amino acid) with score = 115.957 (Figure 1C and D).

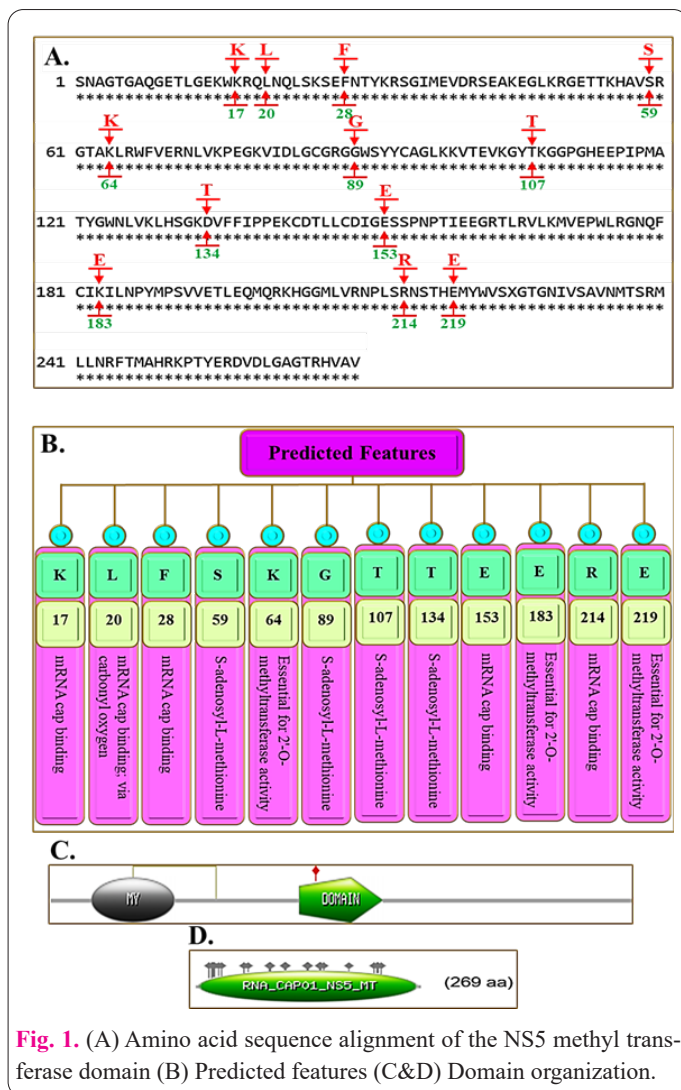


**Fig. 1.** (A) Amino acid sequence alignment of the NS5 methyl transferase domain (B) Predicted features (C&D) Domain organization.

### 3.2. DFT analysis

A comprehensive study combining density functional theory (DFT) and molecular docking was conducted to investigate the reactivity, stability, and potential bioactivity of Isoquercitrin. Chemical structure of Isoquercitrin is shown in Figure 2A. The geometry of Isoquercitrin was optimized to achieve stable conformations, as illustrated in Figure 2B. The analysis focused on frontier molecular orbitals, including the highest occupied molecular orbitals (HOMO), the lowest unoccupied molecular orbitals (LUMO), and the energy gap between them. These parameters provide critical insights into molecular stability and reactivity [21-23]. HOMO acts as an electron donor, while LUMO serves as an electron acceptor. Compounds with smaller HOMO-LUMO energy gaps are generally associated with higher bioactivity, emphasizing variations in reactivity among the studied species [24,25,26]. The calculated energy gap of Isoquercitrin is 3.63 eV, respectively. Figure 2C illustrates the HOMO, LUMO, and energy gaps for this compound.

### 3.3. Molecular Electrostatic Potential map

The molecular electrostatic potential (MEP) provides a visual depiction of the distribution of positive and negative charges on molecular surfaces. The charge distribution is represented by different colors: red denotes regions of high negative potential, blue indicates areas of high positive potential, and green and yellow correspond to intermediate potentials [27,28]. Regions with red coloration, associated

with negative potential, are more susceptible to electrophilic attacks, while blue regions, with positive potential, are more likely to undergo nucleophilic attacks. Intermediate colors signify a balance between these tendencies. The MEP of Isoquercitrin was calculated and is presented in Figure 3. The computed potential value of  $-9.662 \times 10^{-2}$  indicates that Isoquercitrin exhibits significant negative potential. Detailed analysis shows that red regions, indicating greater susceptibility to electrophilic attack, are primarily located around oxygen atoms, while yellow areas suggest potential sites for nucleophilic interactions.

### 3.4. ADMET analysis

These properties are critical in drug development, providing insights into how a compound enters the bloodstream, distributes through tissues, undergoes metabolic transformations, and is ultimately excreted. Such predictions are particularly valuable during the early stages of drug discovery. The absorption phase evaluates parameters such as Caco-2 permeability, MDCK permeability, Pgp-inhibition, Pgp-substrate properties, human intestinal absorption (HIA), and oral bioavailability at F20% and F30%. The Caco-2 cell line, derived from human colon adenocarcinoma cells, is a standard model for assessing drug permeability. Its permeability is expressed as the logarithm of centimeters per second ( $\log \text{ cm/s}$ ), where values above  $-5.15 \log \text{ cm/s}$  indicate favorable permeability. Similarly, MDCK cells, commonly used to measure absorption and

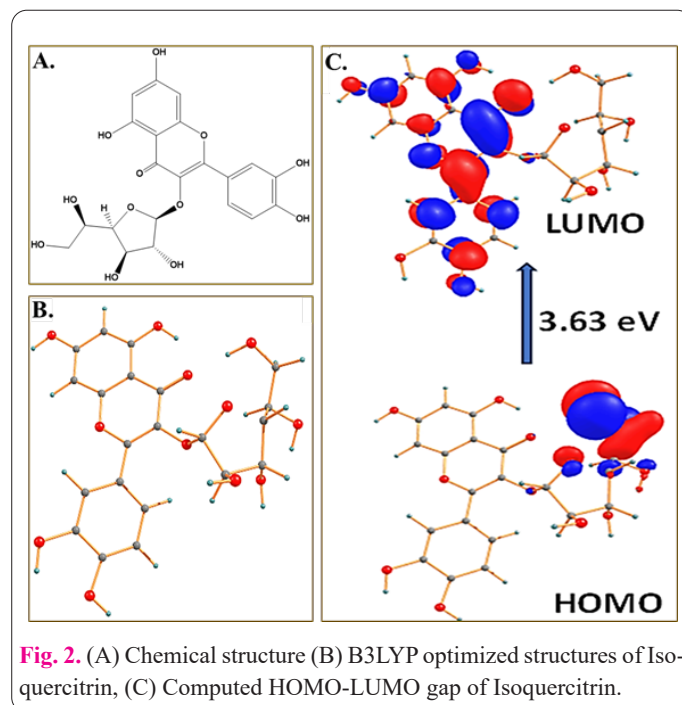


**Fig. 2.** (A) Chemical structure (B) B3LYP optimized structures of Isoquercitrin, (C) Computed HOMO-LUMO gap of Isoquercitrin.

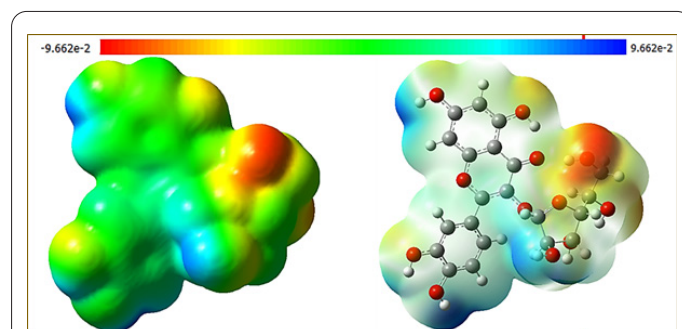


**Fig. 3.** B3LYP computed MEPs of Isoquercitrin.

blood-brain barrier penetration, evaluate permeability through the apparent permeability coefficient (Papp) in cm/s. Values exceeding  $2 \times 10^{-6}$  cm/s are considered indicative of high permeability [29].

A Pgp-inhibitor is a compound that blocks the function of P-glycoprotein, a transporter protein responsible for recognizing and exporting various xenobiotics, many of which are also substrates of CYP3A4. The likelihood of a compound being a Pgp-inhibitor is scored on a scale from 0 to 1: values between 0 and 0.3 indicate strong inhibition, 0.3 to 0.7 signify moderate inhibition, and 0.7 to 1.0 reflect weak inhibition (++) . Modulating P-glycoprotein activity can substantially affect the pharmacokinetics of Pgp-recognized compounds, influencing their therapeutic efficacy or potential contraindications. Similarly, the probability of a compound being a Pgp substrate is rated from 0 to 1. Scores between 0 and 0.3 suggest a high likelihood of being a substrate, 0.3 to 0.7 indicate moderate likelihood and 0.7 to 1.0 imply low likelihood. Human intestinal absorption (HIA) is a critical parameter for evaluating the effectiveness of orally administered drugs. A strong correlation exists between oral bioavailability and intestinal absorption, making HIA a reliable predictor of bioavailability. Molecules with absorption below 30% are typically considered poorly absorbed. The HIA score, ranging from 0 to 1, indicates the likelihood of intestinal absorption: scores between 0 and 0.3 reflect excellent absorption, 0.3 to 0.7 indicate moderate absorption, and 0.7 to 1.0 suggest poor absorption.

F20% is an essential parameter for assessing oral drugs, representing the likelihood of achieving 20% oral bioavailability—a key indicator of a drug's effectiveness in systemic delivery. The F20% probability score, ranging from 0 to 1, categorizes this likelihood: scores from 0 to 0.3 indicate excellent probability, 0.3 to 0.7 reflect medium probability, and 0.7 to 1.0 (++) rating signify poor probability. Similarly, F30% evaluates the likelihood of achieving 30% oral bioavailability, a crucial benchmark for systemic circulation effectiveness. Molecules with bioavailability exceeding 30% are deemed effective (F30%-). The F30% probability score, also on a 0 to 1 scale, follows the same categorization: 0 to 0.3 for excellent probability, 0.3 to 0.7 for medium probability, and 0.7 to 1.0 for poor probability (++) .

Drug distribution encompasses parameters such as Plasma Protein Binding (PPB), Volume of Distribution (VD), Blood-Brain Barrier (BBB) penetration, and Fraction Unbound (Fu). Plasma Protein Binding (PPB) significantly influences a drug's uptake and distribution, as it affects the proportion of free drugs available for therapeutic action. High PPB values, typically above 90%, can reduce the drug's effectiveness by limiting the active free concentration. An optimal PPB value is below 90% to maintain a suitable therapeutic index. Volume of Distribution (VD), expressed in liters per kilogram (L/kg), measures the extent of a drug's distribution throughout the body. It provides insights into tissue distribution and the pharmacokinetic profile, with appropriate VD values generally ranging between 0.04 and 20 L/kg. Blood-brain barrier (BBB) penetration is crucial for drugs targeting the central nervous system (CNS), determining whether the drug can effectively reach its active site. BBB penetration, measured in centimeters per second (cm/s), is classified as excellent (0 to 0.3), medium (0.3 to 0.7), or poor (++)

rating, 0.7 to 1.0). Drugs in plasma exist in bound and unbound forms. Binding to plasma proteins reduces the concentration of the free, active form of the drug, thereby impacting its therapeutic efficacy. A balance between bound and unbound forms is critical for achieving optimal pharmacological action.

The Fraction Unbound (Fu) value indicates the proportion of a drug that remains unbound in plasma. Fu values are categorized as high if they exceed 20%, medium if they range between 5% and 20%, and low if they are below 5%. Values of 5% or more are considered excellent, while those below 5% are deemed poor. Drug metabolism is evaluated by examining the inhibition of key cytochrome enzymes, including CYP1A2, CYP2C19, CYP2C9, CYP2D6, and CYP3A4. Metabolism occurs in two phases: phase I (oxidative reactions) and phase II (conjugative reactions). The cytochrome P450 enzyme family, comprising 57 isozymes, is responsible for metabolizing approximately two-thirds of known drugs. Of these, five enzymes—CYP1A2,

**Table 1.** ADMET analysis of isoquercitrin.

Species	Isoquercitrin
MW	464.1
H-bond acceptors	12
H-bond donors	8
Rotatable bond	5
TPSA	210.51
Log S	-3.915
Log P	0.529
Caco-2 Permeability	-6.325
MDCK Permeability	8e-06
Pgp-inhibitor	0.01
Pgp-substrate	0.9689
HIA	0.687
F20%	0.272
F30%	0.998
PPB	88.69%
VD	0.917
BBB Penetration	0.017
Fu	13.78 %
CYP1A2 inhibitor	0.34
CYP2C19 inhibitor	0.021
CYP2C9 inhibitor	0.052
CYP2D6 inhibitor	0.092
CYP3A4 inhibitor	0.118
CL	5.029
T <sub>1/2</sub>	0.823

[MW=Molecular Weight, TPSA= Topological polar surface area, Log S= logarithm of aqueous solubility value, Log P= logarithm of the n-octanol/water distribution coefficient, Caco-2= human colon adenocarcinoma cell lines, MDCK= Madin–Darby Canine Kidney cells, Pgp= P-glycoprotein, HIA= Human intestinal absorption, F20%= human oral bioavailability 20%, F30%= human oral bioavailability 30%, PPB= Plasma protein binding, VD=Volume Distribution, BBB= blood–brain barrier, Fu= fraction unbound, CL= clearance of a drug, T<sub>1/2</sub>= half-life of a drug. For the classification endpoints, the prediction probability values are transformed into six symbols: 0-0.1(--), 0.1-0.3(--), 0.3-0.5(-), 0.5-0.7(+), 0.7-0.9(++), 0.9-1(+++)].

CYP3A4, CYP2C9, CYP2C19, and CYP2D6—account for 80% of drug metabolism. The likelihood of enzyme inhibition is expressed as a probability value ranging from 0 to 1. Excretion is assessed through drug clearance (CL) and half-life ( $T_{1/2}$ ). Clearance, a critical determinant of drug effectiveness, is measured in milliliters per minute per kilogram (ml/min/kg). High clearance is defined as a value exceeding 15 ml/min/kg, moderate clearance ranges from 5 to 15 ml/min/kg, and low clearance falls below 5 ml/min/kg. A clearance value of 5 ml/min/kg or higher is generally considered excellent, while values below this threshold are poor. The half-life ( $T_{1/2}$ ) reflects the time required for the drug's concentration in the body to decrease by half, influenced by both clearance and volume of distribution. The half-life is classified on a scale from 0 to 1, where 0 to 0.3 indicates excellent, 0.3 to 0.7 represents medium, and 0.7 to 1.0 (++) rating signifies poor.

The ADME analysis results are summarized in Table 1.

Isoquercitrin exhibits the following properties: it has twelve hydrogen bond acceptors, eight hydrogen bond donors, and five rotatable bonds. Absorption analysis indicates excellent Caco-2 permeability (-6.325), P-glycoprotein (Pgp) shows good inhibition (0.01), and moderate potential as a Pgp substrate (0.9689). Human intestinal absorption (HIA), along with fraction absorbed at 20% (F20%) and 30% (F30%), is excellent (0–0.1). Distribution analysis reveals optimal plasma protein binding (PPB) at 88.69%, excellent volume of distribution (VD), and effective blood-brain barrier (BBB) penetration. The fraction unbound ( $F_u$ ) is moderate at 13.78%. Metabolism analysis shows that Isoquercitrin strongly inhibits CYP2C9, CYP2C19, CYP3A4, CYP1A2 and CYP2D6. Excretion analysis reveals moderate clearance (CL) at 5.029 ml/min/kg and a long half-life ( $T_{1/2}$ ) of 0.823.

### 3.5. Molecular docking analysis

The molecular docking analysis revealed specific interactions between the Isoquercitrin and the amino acid residues of the target protein {Dengue virus 1 NS5 Methyltransferase (5IKM)} [30]. After calculating Gasteiger charges of each atom of the molecule and total energy, the charged protein was saved as a PDBQT file. Prior to docking, water molecules were removed, and the grid box was defined with dimensions  $30 \times 30 \times 30 \text{ \AA}$ , centered at coordinates  $X = 9.339$ ,  $Y = 23.565$ ,  $Z = 24.355$ , encompassing the residues of the protein's active site. The docked models were evaluated to determine binding affinities and the nature of intermolecular interactions between Isoquercitrin and the protein. By analysing preferred binding orientations, a variety of ligand-protein interactions were identified. Compound demonstrating strong interactions with the target protein was considered effective in the docking process.

The study confirmed that Isoquercitrin established binding interactions with the target protein. Figure 4 presents 3D and 2D visualizations of the ligand-protein interactions for Isoquercitrin. Binding affinity values across nine binding modes were recorded as -9.7, -9.3, -9.2, -9.0, -8.9, -8.9, -8.8, -8.8, and -8.6 kcal/mol. The conformation with the most negative binding energy (-9.7 kcal/mol) represents the highest binding affinity. Key interactions for Isoquercitrin include hydrogen bonding, carbon-hydrogen bonds, and  $\pi$ -sigma and  $\pi$ -alkyl interactions. This study emphasizes the critical roles of hydrogen bonding,  $\pi$ -alkyl,

and  $\pi$ -sigma interactions in stabilizing the ligand-protein complexes.

## 4. Discussion

The possible therapeutic profits of isoquercitrin, a flavonoid glycoside, have warranted care to its examination, particularly in the fight in contradiction of viral infections. Isoquercitrin conjugated aromatic ring system & hydroxyl groups are two crucial appearances exposed through its electrical structure & contribute to its biological action. These structural components suggestively influence its antiviral, anti-inflammatory, & antioxidant qualities. The electronic structure of isoquercitrin marks its capacity to interact with biological targets through making it informal to attach to proteins & enzymes concerned in disease processes, like the Dengue virus 1 NS5 methyltransferase.

The absorption, distribution, metabolism, and excretion (ADME) characteristics of isoquercitrin are important to its potential as a medicinal agent. As an auspicious option for therapeutic progress, isoquercitrin has a satisfactory bioavailability & is absorbed resourcefully. Its metabolic routes & any interactions with other drugs, however, are necessary to be considered further.

The title compound was optimized using the DFT/B3LYP/6-31g level of theory, providing valuable insights into its stability and reactivity. Based on the computed energy gap, selected compound emerged as the reactive with computed energy gap of 3.63 eV. Molecular electrostatic potential (MEP) maps indicated that Isoquercitrin exhibits the negative potential region. The calculated binding energy for the docked compound was -9.7 kcal/mol. This negative value indicates strong protein-binding potential of Isoquercitrin. Key interactions, including hydrogen bonding,  $\pi$ -alkyl, and  $\pi$ -sigma interactions, play crucial roles in stabilizing the binding of these compounds to the protein. Isoquercitrin primarily engages in hydrogen bonding and  $\pi$ -alkyl interactions. This analysis underscores the importance of specific interactions—such as hydrogen bonding,  $\pi$ -alkyl, and  $\pi$ -sigma forces in facilitating strong ligand-protein binding and highlights the good binding efficiency of Isoquercitrin.

The ADME analysis of Isoquercitrin offers valuable insights into its unique properties and potential applications. It exhibits excellent permeability, distribution, and metabolic stability, positioning it as a strong candidate for further research. Meanwhile, Isoquercitrin shows strong P-glycoprotein inhibition and notable distribution and metabolism-related characteristics. These ADME profiles are critical for assessing the pharmacokinetic potential of the compounds and their suitability for therapeutic applications. Further research into these properties is expected to inform drug development and influence future therapeutic strategies.

### 4.1. Importance of the research and current trends:

The research on dengue virus (DENV) NS5 methyltransferase (MTase) as a therapeutic target is critical due to the increasing global prevalence of mosquito-borne diseases and the absence of effective antiviral treatments. With millions of dengue cases annually, targeting the highly conserved NS5 protein, which plays a vital role in viral replication and immune evasion, holds significant promise for broad-spectrum antiviral therapies [31].

## 4.2. Importance of the research

The study highlights the potential of Isoquercitrin, a natural flavonoid, as a promising inhibitor of NS5 MTase. This compound's chemical structure and pharmacokinetic properties have been evaluated using advanced computational techniques, including molecular docking and Density Functional Theory (DFT) [36]. Molecular docking studies, such as those that identified inhibitors for Japanese Encephalitis Virus proteins, demonstrate the versatility of these methods in antiviral drug discovery [32-42].

Research on the gene expression profiling and functional annotation of dengue virus proteins further strengthens the understanding of the molecular mechanisms underlying its pathogenicity. Such investigations provide a solid foundation for designing targeted antiviral interventions [38]. Moreover, studies focusing on methyltransferase activity in DENV RNA viruses showcase the critical role of this enzyme in the viral lifecycle and highlight it as a viable drug target [37].

Structural studies on protein microtubules, particularly at the nano-scale level, contribute valuable insights into cellular mechanics and drug interactions. For instance, the analysis of microtubule buckling and vibrational properties offers guidance for designing drugs that disrupt viral replication without compromising cellular integrity [41]. Investigations into thermal stress effects on microtubules also provide a foundation for understanding how cellular mechanics are affected under disease conditions, which may influence future therapeutic strategies [35].

## Acknowledgment

This project was funded by the Deanship of Scientific Research (DSR) at King Abdulaziz University, Jeddah, under grant no. (GPIP: 1471-665-2024). The authors, therefore, acknowledge with thanks DSR for technical and financial support.

## References

- Bhatt S, Gething PW, Brady OJ, Messina JP, Farlow AW, Moyes CL, Drake JM, Brownstein JS, Hoen AG, Sankoh O (2013) The global distribution and burden of dengue. *Nature* 496(7446):504–507. doi: 10.1038/nature12060
- Wilson ME, Chen LH (2015) Dengue: update on epidemiology. *Curr Infect Dis Rep* 17:1–8. doi: 10.1007/s11908-014-0457-2
- Mackenzie JS, Gubler DJ, Petersen LR (2004) Emerging flaviviruses: the spread and resurgence of Japanese encephalitis, West Nile and dengue viruses. *Nat Med* 10(Suppl 12):S98–S109. doi: 10.1038/nm1144
- Casseb SMM, Melo KFL, Carvalho CAM, Santos CRD, Franco ECS, Vasconcelos PFDC (2023) Experimental Dengue Virus Type 4 Infection Increases the Expression of MicroRNAs-15/16, Triggering a Caspase-Induced Apoptosis Pathway. *Curr Issues Mol Biol* 45(6):4589–4599. doi: 10.3390/cimb45060291
- Egloff M-P, Decroly E, Malet H, Selisko B, Benarroch D, Ferron F, Canard B (2007) Structural and Functional Analysis of Methylation and 5'-RNA Sequence Requirements of Short Capped RNAs by the Methyltransferase Domain of Dengue Virus NS5. *J Mol Biol* 372(3):723–736. doi: 10.1016/j.jmb.2007.07.005
- Issur M, Geiss BJ, Bougie I, Picard-Jean F, Despains S, Mayette J, Hobdey SE, Bisaiillon M (2009) The flavivirus NS5 protein is a true RNA guanylyltransferase that catalyzes a two-step reaction to form the RNA cap structure. *RNA* 15(12):2340–2350. doi: 10.1261/rna.1609709
- Singh U, Singh D, Singh M, Maurya S, Srivastava J, Singh R, Singh S (2004) Characterization of phenolic compounds in some Indian mango cultivars. *Int J Food Sci Nutr* 55(2):163–169. doi: 10.1080/09637480410001666441
- Kucuk C (2023) Synthesis, characterization, DFT studies, and molecular docking investigation of silver nitrate complex of 5-benzimidazole carboxylic acid as targeted anticancer agents. *J Mol Struct* 1293:136166. doi: 10.1016/j.molstruc.2023.136166
- Robert HM, Usha D, Amalanathan M, Geetha RRJ, Mary MSM (2021) Vibrational spectral, density functional theory and molecular docking analysis on 4-nitrobenzohydrazide. *J Mol Struct* 1223:128948. doi: 10.1016/j.molstruc.2020.128948
- Uzun S, Esen Z, Koç E, Usta NC, Ceylan M (2019) Experimental and density functional theory (MEP, FMO, NLO, Fukui functions) and antibacterial activity studies on 2-amino-4-(4-nitrophenyl)-5,6-dihydrobenzo[h]quinoline-3-carbonitrile. *J Mol Struct* 1178:450–457. doi: 10.1016/j.molstruc.2018.10.001
- Frisch M, Trucks G, Schlegel H, Scuseria G, Robb M, Cheeseman J, Scalmani G, Barone V, Petersson G, Nakatsuji H (2016) Gaussian 16, Revision C.01. Gaussian, Inc., Wallingford CT.
- Becke AD (1992) Density-functional thermochemistry. I. The effect of the exchange-only gradient correction. *J Chem Phys* 96(3):2155–2160. doi: 10.1063/1.462066
- Ditchfield R, Hehre WJ, Pople JA (1971) Self-consistent molecular-orbital methods. IX. An extended Gaussian-type basis for molecular-orbital studies of organic molecules. *J Chem Phys* 54(2):724–728. doi: 10.1063/1.1674902
- Dennington R, Keith T, Millam J (2019) GaussView, Version 6.1.1. Semichem Inc., Shawnee Mission KS.
- Paul Gleeson M, Hersey A, Hannongbua S (2011) In-silico ADME models: a general assessment of their utility in drug discovery applications. *Curr Top Med Chem* 11(4):358–381. doi: 10.2174/156802611794480927
- Xiong G, Wu Z, Yi J, Fu L, Yang Z, Hsieh C, Yin M, Zeng X, Wu C, Lu A (2021) ADMETlab 2.0: an integrated online platform for accurate and comprehensive predictions of ADMET properties. *Nucleic Acids Res* 49(W1):W5–W14. doi: 10.1093/nar/gkab255
- Pagadala NS, Syed K, Tuszyński J (2017) Software for molecular docking: a review. *Biophys Rev* 9:91–102. doi: 10.1007/s12551-016-0247-1
- Azam M, Barik SR, Mohapatra PK, Kumar M, Ansari A, Mohapatra RK, Trzesowska-Kruszynska A, Al-Resayes SI (2023) A Bowl-Shaped Zinc-Salen Complex: Structural Analysis and Molecular Docking Studies against Omicron-S and Delta-S

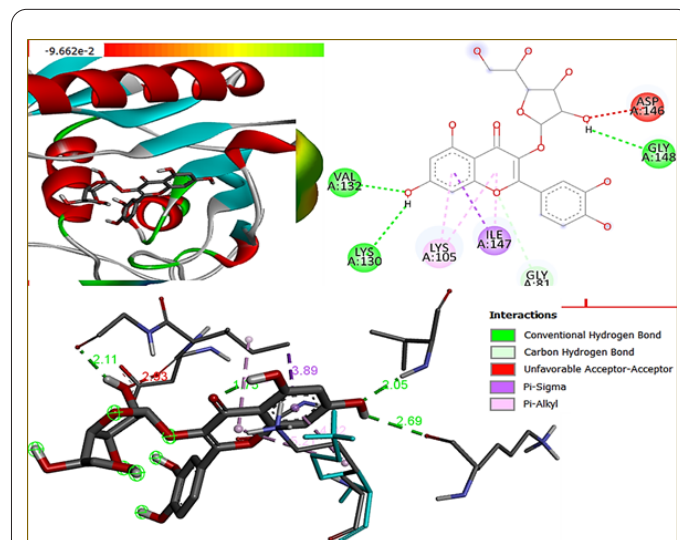


**Fig. 4.** 3D and 2D structures showing interactions between amino acid residues and Isoquercitrin.

- Variants. *Russ J Inorg Chem* 68(8):1005–1012. doi: 10.1134/S0036023623600740
19. Trott O, Olson AJ (2010) AutoDock Vina: improving the speed and accuracy of docking with a new scoring function, efficient optimization, and multithreading. *J Comput Chem* 31(2):455–461. doi: 10.1002/jcc.21334
20. Biovia DS (2021) Discovery Studio Visualizer 4.5. Dassault Systèmes, San Diego.
21. Ahmed M, Gupta MK, Ansari A (2023) DFT and TDDFT exploration on the role of pyridyl ligands with copper toward bonding aspects and light harvesting. *J Mol Model* 29(11):358. doi: 10.1007/s00894-023-05765-4
22. Ahmed M, Malhotra SS, Yadav O, Monika, Saini C, Sharma N, Gupta MK, Mohapatra RK, Ansari A (2024) DFT and TDDFT exploration on electronic transitions and bonding aspect of DPA and PTDC ligated transition metal complexes. *J Mol Model* 30(5):122. doi: 10.1007/s00894-024-05912-5
23. Malhotra SS, Kumar M, Gupta MK, Ansari A (2024) Theoretical exploration of copper-based electrolytes for third-generation dye-sensitized solar cells. *Mater Today Commun* 39:109208. doi: 10.1016/j.mtcomm.2024.109208
24. Świsłocka R, Regulska E, Karpińska J, Świdorski G, Lewandowski W (2019) Molecular structure and antioxidant properties of alkali metal salts of rosmarinic acid. Experimental and DFT studies. *Molecules* 24(14):2645. doi: 10.3390/molecules24142645
25. Mohapatra RK, Azam M, Mohapatra PK, Sarangi AK, Abdalla M, Perekhoda L, Yadav O, Al-Resayes SI, Jong-Doo K, Dhama K, Ansari A, Seidel V, Verma S, Raval MK (2022) Computational studies on potential new anti-Covid-19 agents with a multi-target mode of action. *J King Saud Univ Sci* 34(5):102086. doi: 10.1016/j.jksus.2022.102086
26. Yadav O, Ansari M, Ansari A (2021) Electronic structures, bonding, and energetics of non-heme mono and dinuclear iron-TPA complexes: a computational exploration. *Struct Chem* 32(5):2007–2018. doi: 10.1007/s11224-021-01775-1
27. Reed AE, Curtiss LA, Weinhold F (1988) Intermolecular interactions from a natural bond orbital, donor-acceptor viewpoint. *Chem Rev* 88(6):899–926. doi: 10.1021/cr00088a005
28. Dong J, Wang N-N, Yao Z-J, Zhang L, Cheng Y, Ouyang D, Lu A-P, Cao D-S (2018) ADMETlab: a platform for systematic ADMET evaluation based on a comprehensively collected ADMET database. *J Cheminf* 10:1–11. doi: 10.1186/s13321-018-0283-x
29. Sahu R, Mohapatra RK, Al-Resayes SI, Das D, Parhi PK, Rahman S, Pintilie L, Kumar M, Azam M, Ansari A (2021) An efficient synthesis towards the core of Crinipellin: TD-DFT and docking studies. *J Saudi Chem Soc* 25(2):101193. doi: 10.1016/j.jscs.2020.101193
30. Ahamad MN, Shahid M, Ansari A, Kumar M, Khan IM, Ahmad M, Arif R (2019) A combined experimental and theoretical approach to investigate the structure, magnetic properties and DNA binding affinity of a homodinuclear Cu(ii) complex. *New J Chem* 43(19):7511–7519. doi: 10.1039/C9NJ00228F
31. Patel A, El-Gamal B, Abd Ellatif M, Alotheid H, Mirdad TM, Almalki WH, Alwabli AS (2022) Unraveling activity of crucial domain HABD protein in dengue virus. *Cell Mol Biol* 68(4):66–74. doi: 10.14715/cmb/2022.68.4.11
32. Alwabli AS (2023) Fluorescence emission and molecular docking studies identified Novobiocin as a potent inhibitor of the Japanese Encephalitis Virus (JEV) envelope protein. *Int J Pharm Investig* 13(2). doi: 10.4103/jpi.jpi\_13\_23. Doi. 10.5530/ijpi.13.2.042
33. Alwabli AS (2022) Comparative evaluation of dengue virus (DENV) serotypes infections in humans (*Homo sapiens*). *Int J Pharm Investig* 12(4). doi: 10.4103/jpi.jpi\_12\_22. Doi. 10.5530/ijpi.2022.4.83
34. Alwabli AS (2022) Lead identification against 3C-like protease of SARS-CoV-2 via target-based virtual screening and molecular dynamics simulation. *J Young Pharm* 14(2):179. doi: 10.4103/jyp.jyp\_14\_22. DOI: 10.5530/jyp.2022.14.34
35. Alhebshi AMS, Metwally AM, Al-Basyouni KS, Mahmoud SR, Al-Solami HM, Alwabli AS (2022) Biomechanical behavior of protein microtubules in living cells using the nonlocal beam theory. *Phys Mesomech* 25(2). <https://doi.org/10.1134/S1029959922020096>
36. Alwabli AS, Qadri I (2021) Identification of possible inhibitor molecule against NS5 MTase and RdRp protein of dengue virus in Saudi Arabia. *Indian J Pharm Educ Res* 55(4):1028–1036. DOI: 10.5530/ijper.55.4.203
37. Alwabli AS, Alattas SG, Mohammed N, Alhebshi A, Alkenani N, Al-ghmady K, Qadri I (2019) Methyltransferase activity of Dengue RNA virus by using purified protein. *Int J Drug Dev Res* 11(1). DOI: 10.36648/0975-9344.11.2.131
38. Taj M, Khadimallah MA, Hussain M, Fareed K, Safeer M, Khedher KM, Ahmad M, Naeem MN, Qazaq A, Al Qahtani A, Mahmoud SR, Alwabli AS, Tounsi A (2021) Thermal stress effects on microtubules based on orthotropic model: Vibrational analysis. *Advances in Concrete Construction* 11(3):255–260. <https://doi.org/10.12989/acc.2021.11.3.255>
39. Alwabli AS, Al-Attas SG, Mohammed N, Alhebshi A, Alkenani N, Al-ghmady K, Qadri I (2019) Molecular docking analysis of netropsin and novobiocin with the viral protein targets HABD, MTD, and RCD. *Bioinformatics* 15(4):233–239. doi: 10.6026/97320630015233
40. Malik A, Afaq S, Alwabli AS, Al-ghmady K (2019) Networking of predicted post-translational modification (PTM) sites in human EGFR. *Bioinformatics* 15(7):448–455. doi: 10.6026/97320630015448
41. Alwabli AS, Kaci A, Bellifa H, Bousahla AA, Tounsi A, Alzahrani DA, Abulfaraj AA, Bourada F, Benrahou KH, Tounsi A, Mahmoud SR, Hussain M (2021) The nano-scale buckling properties of isolated protein microtubules based on modified strain gradient theory and a new single variable trigonometric beam theory. *Adv Nano Res* 10(1):15–24. <https://doi.org/10.12989/anr.2021.10.1.015>
42. Alwabli AS "Deciphering the molecular landscape of dengue infection: Insights from gene expression profiling and Protein Interactions" *The Microbe*, Vol. 5: pp. 100195, (2024). <https://doi.org/10.1016/j.microb.2024.100195>